

Three-Dimensional Wave Packet Approach for the Quantum Transport of Atoms through Nanoporous Membranes

Alfonso Gijón, José Campos-Martínez, and Marta I. Hernández*

*Instituto de Física Fundamental, Consejo Superior de Investigaciones Científicas
(IFF-CSIC), Serrano 123, 28006 Madrid, Spain*

E-mail: marta@iff.csic.es

Abstract

Quantum phenomena are relevant to the transport of light atoms and molecules through nanoporous two-dimensional (2D) membranes. Indeed, confinement provided by (sub-)nanometer pores enhances quantum effects such as tunneling and zero point energy (ZPE), even leading to quantum sieving of different isotopes of a given element. However, these features are not always taken into account in approaches where classical theories or approximate quantum models are preferred. In this work we present an exact three-dimensional wave packet propagation treatment for simulating the passage of atoms through periodic 2D membranes. Calculations are reported for the transmission of ^3He and ^4He through graphdiyne as well as through a holey graphene model. For He-graphdiyne, estimations based on tunneling-corrected transition state theory are correct: both tunneling and ZPE effects are very important but competition between each other leads to a moderately small $^4\text{He}/^3\text{He}$ selectivity. Thus, formulations that neglect one or another quantum effect are inappropriate. For the transport of He isotopes through leaky graphene, the computed transmission probabilities are highly

structured suggesting widespread selective adsorption resonances and the resulting rate coefficients and selectivity ratios are not in agreement with predictions from transition state theory. Present approach serves as a benchmark for studies of the range of validity of more approximate methods.

KEYWORDS: quantum sieving, nanoporous two-dimensional materials, Helium isotopes, graphdiyne, zero point energy, tunneling

Recent progress in the fabrication of nanoporous two-dimensional (2D) membranes has led to propose them as efficient sieves at the molecular level.¹⁻³ Particularly, it has been suggested that these membranes could be used for the separation of a specific isotope within an atomic or molecular gas,^{4,5} a process which is both important and challenging. For example, ³He is essential to several applications ranging from security to basic research but it is very rare and its growing demand is leading to an acute shortage of this species.^{6,7} Moreover, separation of ³He from the much more abundant ⁴He -in turn, commonly extracted from natural gas- usually involves very expensive cryogenic methods. Separation of the heavier isotopes of H₂ is also crucial for various technologies.⁸ Ideally, single-layer membranes should involve a low energy consumption and efficiency, provided that the pores are designed to optimize the desired separation process.

For sufficiently low pressures, the study of purification of a gas mixture can be modeled by the dynamics of an atom or molecule passing through a pore of the 2D membrane. In this way, rate coefficients for the transmission of the isotopic species of the mixture, say k_a and k_b , are independently computed at a given temperature T , and the efficiency for the isotope separation is estimated by means of the selectivity ratio $S_{a/b}(T) = k_a(T)/k_b(T)$. Since isotopes are chemically identical, the separation mechanism must be provided by mass-dependent dynamical effects. At sufficiently low temperatures, quantum effects may entail large selectivity ratios as compared with those based on classical diffusion, for instance. Recently, a rather large number of works have shown that quantum tunneling might rule an efficient separation process.^{5,9-14} However, these studies are based on one-dimensional (1D) quantum-mechanical calculations, whereas the molecular motion actually occurs in the three-dimensional (3D) space where differences between the quantum energy levels of the isotopes confined within the pores can also lead to quantum sieving.¹⁵ These effects, which may be generally termed as zero point energy (ZPE) effects,¹⁶ have been invoked in various theoretical^{2,17-19} and experimental^{20,21} works on porous materials. It is worth to emphasize that tunneling and ZPE effects work in opposite directions: while tunneling

favors the passage of lighter molecules, ZPE increases the transmission of the heavier ones since their smaller ZPE is associated to a smaller “effective size”. Therefore, it is important to evaluate the relative role of each effect on the systems of interest.

We have recently studied²² the interplay between tunneling and ZPE effects in the transmission of He isotopes through graphdiyne,^{23,24} a promising new material for molecular separation applications^{11,25–27} as it exhibits regularly distributed pores of sub-nanometer size. To this end we relied on transition state theory (TST) with specific inclusion of reaction-path tunneling corrections. He-graphdiyne interactions were represented by a force field validated from *ab initio* electronic structure calculations.¹¹ It was found that, if only tunneling effects are considered (ignoring ZPE), ³He transmission rate is larger than the ⁴He one in the studied 20-100 K temperature range, reaching a selectivity factor of ≈ 2.5 at 20 K. This result is similar to findings accomplished from 1D calculations on related systems.⁹ However, the complete theory, which also includes ZPE effects, leads to a *qualitatively* different conclusion: transport becomes more probable for ⁴He and at 20 K the selectivity ratio is also ≈ 2.5 but this time favoring ⁴He instead of ³He. It became clear that the transmission of atoms through the membrane must be studied within a 3D model and that accurate quantum calculations may be needed in order to properly account for the delicate competition between the above mentioned quantum effects.

Here we present an accurate quantum-mechanical formulation to study the transmission of an atom through a periodic 2D membrane, therefore going beyond TST. The time-dependent Schrödinger equation is solved by propagating 3D wave packets and, from the calculation of the flux through a surface separating the incident and transmitted wave packets, transmission probabilities and rate coefficients are obtained. Time-dependent quantum-mechanical methods have been extensively applied to various collisional and photodissociation processes^{28,29} but, although one of their first applications was devoted to the scattering of atoms by surfaces,³⁰ we are not aware of a generalization of this approach to the scattering by a porous membrane. Present 3D wave packet method (WP3D in short) is applied to

He-graphdiyne¹¹ as well as to a holey graphene model.³¹ The goal of this work is to provide with a trustworthy method for the investigation of quantum phenomena in the transport of atoms through membranes, in this way allowing us the assessment of more approximate treatments. It is found that TST is reliable for He-graphdiyne but not for He-holey graphene. Furthermore, it turns up that in addition to tunneling and ZPE effects, selective adsorption resonances³²⁻³⁴ (another genuine quantum feature) can also play a role in these processes. It is expected that this research will serve to uncover new clues for the design of optimal pores for quantum sieving.

The rest of the paper arranges as follows. First we give the theory for the transmission of a 3D wave packet through a periodic membrane, accompanied by a refresher outline of TST. Results are presented and discussed first for He-graphdiyne, followed by He-holey graphene. The report ends with a conclusion paragraph.

Theory. In the present WP3D approach we consider the scattering of an atom of mass μ by a periodic membrane by means of time-dependent 3D wave packet methods.^{35,36} The membrane coincides with the xy plane of the reference frame, whose origin is set at the center of one of its pores; hence the position of the atom is given by $\mathbf{r} = (\mathbf{R}, z)$, z being the distance to the membrane plane and $\mathbf{R} = (x, y)$. The wave packet representing the atom is discretized on a grid of evenly spaced \mathbf{r} points and at the start of the propagation is given as a product of a Gaussian wave packet³⁷ in z times a plane wave with wave vector \mathbf{K} in \mathbf{R} . Thus, as in the original work by Yinnon and Kosloff,³⁰ the periodicity of the system is fully exploited by matching the size of the (x, y) grid to that of the unit cell, (Δ_x, Δ_y) , while the values of the parallel wave vector \mathbf{K} are restricted such that the initial plane wave is commensurate with the membrane lattice. The wave packet is propagated in time subject to the time-dependent Schrödinger equation, using the Split Operator method,³⁵ and is being absorbed in the asymptotic regions by means of a wave packet splitting algorithm.³⁸ To obtain the probability of transmission of the atom through the membrane, it is convenient to write first the asymptotic behavior of the stationary wave function for a translational

energy $E = \frac{\hbar^2 k^2}{2\mu}$,

$$\begin{aligned}
\Psi_E^+(\mathbf{r}) &\xrightarrow{z \rightarrow \infty} \sqrt{\frac{\mu}{2\pi\Delta_x\Delta_y\hbar^2}} \left[\frac{e^{i\mathbf{k}\cdot\mathbf{r}}}{\sqrt{-k_z}} + \sum_{\mathbf{G}} A_{\mathbf{G}}^+ \frac{e^{i[k_{z,\mathbf{G}}^+ z + (\mathbf{K}+\mathbf{G})\cdot\mathbf{R}]}}{\sqrt{k_{z,\mathbf{G}}^+}} \right] \\
&\xrightarrow{z \rightarrow -\infty} \sqrt{\frac{\mu}{2\pi\Delta_x\Delta_y\hbar^2}} \sum_{\mathbf{G}} A_{\mathbf{G}}^- \frac{e^{i[k_{z,\mathbf{G}}^- z + (\mathbf{K}+\mathbf{G})\cdot\mathbf{R}]}}{\sqrt{-k_{z,\mathbf{G}}^-}}, \tag{1}
\end{aligned}$$

which represents an incident plane wave with a wave vector $\mathbf{k} = (k_z, \mathbf{K})$ and a set of reflected (+) and transmitted (-) waves with amplitudes $A_{\mathbf{G}}^{\pm}$ labeled by the reciprocal lattice vector, \mathbf{G} . Note that the parallel wave vectors of these waves obey the Bragg condition whereas the perpendicular one is modified to satisfy the conservation of energy, $k_{z,\mathbf{G}}^{\pm} = \pm [k^2 - (\mathbf{K} + \mathbf{G})^2]^{1/2}$, as energy exchange with the membrane is neglected in the present approach. This function is normalized as $\langle \Psi_E^+ | \Psi_{E'}^+(\mathbf{r}) \rangle = \delta(E - E')$. It can be shown that the (total) transmission probability, which is the sum of the squared transmission amplitudes, can be also obtained from the flux of the stationary wave function through a surface $z = z_f$ separating transmitted from incident and reflected waves,³⁹

$$\begin{aligned}
P_{trans}(E) &= \sum_{\mathbf{G}} |A_{\mathbf{G}}^-|^2 \\
&= \frac{2\pi\hbar^2}{\mu} \text{Im} \left(\int dx dy \Psi_E^{+*}(x, y, z_f) \frac{d\Psi_E^+}{dz} \Big|_{z=z_f} \right). \tag{2}
\end{aligned}$$

We have employed this flux formula for computing P_{trans} , where $\Psi_E^{+*}(x, y, z_f)$ is obtained from the time-energy Fourier transform of the evolving wave packet.^{40,41}

The transmission rate coefficient is then obtained from the integration of $P_{trans}(E)$, properly weighted by the Boltzmann factor:

$$k(T) = \frac{1}{hQ_{trans}} \int e^{-E/(k_B T)} P_{trans}(E) dE, \quad (3)$$

where $Q_{trans} = (2\pi\mu k_B T/h^2)^{3/2}$ is the translational partition function per unit volume. In detail, P_{trans} not only depends on the translational energy but it is also labeled by the parallel wave vector \mathbf{K} . A complete calculation of the rate coefficients should involve averaging over a sufficiently large set of \mathbf{K} values. In this work we have used initial wave packets perpendicularly approaching the membrane ($\mathbf{K}=\mathbf{0}$) and postpone the investigation of effects due the different orientations of the incident wave.

Computational details of the WP3D simulations are provided in the Supporting Information Section.

Rate coefficients computed in this way are compared with those obtained from TST as detailed in Ref.²² In short, it is assumed that the reaction path is a straight line perpendicular to the membrane and crossing the center of the pore, which is the TS. Hence the transmission rate coefficient can be written as^{17,42,43}

$$k_{TST}(T) = \gamma \frac{k_B T}{h} \frac{Q^\ddagger}{Q_{trans}} f_{tunn}(T), \quad (4)$$

where

$$Q^\ddagger = \sum_n e^{-E_n/k_B T} \quad (5)$$

is the TS partition function, E_n being the energy levels of the bound states for the degrees of freedom perpendicular to the reaction path (He in-plane vibrations inside the pore). In addition, $f_{tunn}(T)$ is a correction for tunneling effects along the reaction path.^{22,42,43} Finally, γ is a correction factor (not considered previously) related to the fact that only a fraction of the membrane is effective for permeation⁴⁴ and is defined as

$$\gamma = n_p \frac{A_{eff}}{A_{uc}} \quad (6)$$

where A_{eff} is the pore effective size, A_{uc} is the area of the unit cell and n_p is the number of pores per unit cell. Calculation of A_{eff} is detailed below.

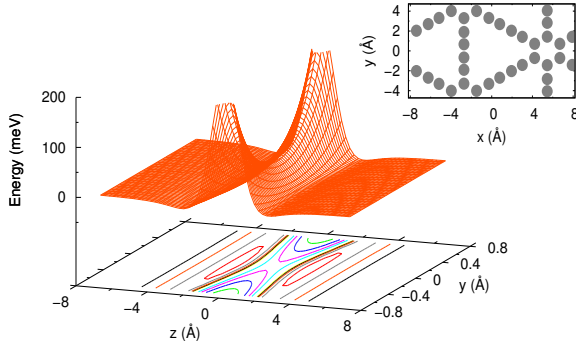


Figure 1: Right-upper panel: Graphdiyne unit cell employed in the WP3D calculations (carbon atoms are depicted by grey filled circles). Left-lower panel: He-graphdiyne interaction potential (meV) as a function of the y and z coordinates, with $x = 0$.

Transmission of He isotopes through graphdiyne. Our first choice for performing WP3D calculations is the transmission of He isotopes through graphdiyne, as for this system a reliable force field has been already obtained¹¹ and TST selectivity ratios showing an involved behavior have been already reported.²² Briefly, the He-graphdiyne potential is obtained as a pairwise sum over He-C pair potentials, the latter being represented by an Improved Lennard-Jones (ILJ) formula⁴⁵ whose parameters have been optimized from comparison with benchmark high level *ab initio* calculations.¹¹ Graphdiyne unit cell is depicted in the right-upper panel of Fig.1 whereas in its left-lower panel a plot of the He-graphdiyne potential is presented. The point $\mathbf{r} = 0$ is a saddle: whereas it corresponds to the maximum of a barrier potential along the “reaction-path” z coordinate -with a height of $E_0 = 36.92$ meV- it is a minimum with respect to displacements along the y and x “in-pore” degrees of freedom. It is worthwhile to note that while the potential barrier is rather low at this saddle point it rapidly rises for paths different to the minimum energy path.

Transmission probabilities for ^4He and ^3He are presented and compared in Fig.2.a). These probabilities rise around 60 meV, a value much higher than the potential barrier (36.9 meV).

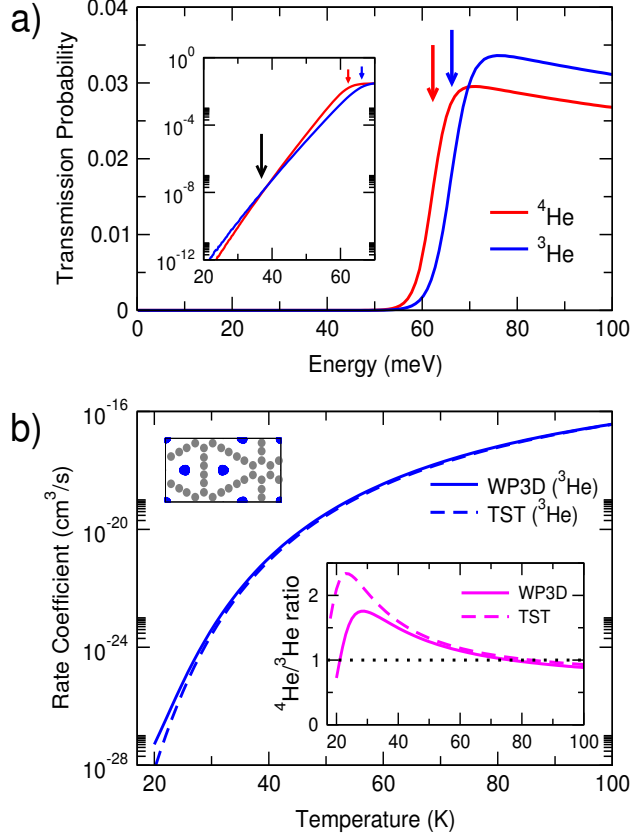


Figure 2: a) WP3D probabilities of ${}^4\text{He}$ and ${}^3\text{He}$ transmission through graphdiyne as a function of the translational energy of the atom (in meV). Red and blue arrows indicate the ${}^4\text{He}$ and ${}^3\text{He}$ reaction thresholds, respectively, as predicted by TST.²² The inset shows these probabilities (in logarithmic scale) for the low energy region. The black arrow shows the potential barrier height. b) ${}^3\text{He}$ WP3D rate coefficients vs. temperature compared with TST estimations. Graphdiyne unit cell, together with the effective area for ${}^3\text{He}$ transmission as obtained from TST (blue spots), are displayed in the upper-left inset. Finally, the ${}^4\text{He}/{}^3\text{He}$ selectivity vs. temperature is presented in the lower-right inset.

The positions of these thresholds agree quite well with the TST prediction, given by the lowest energy levels of Eq. 5, 62.2 and 66.2 meV for ${}^4\text{He}$ and ${}^3\text{He}$, respectively,²² and depicted by arrows in the figure. In addition, it is worth noticing the small value of the probabilities above threshold: they are slightly lower (higher) than 0.03 for ${}^4\text{He}$ (${}^3\text{He}$). These values can be related to the ratio between the effective size of the pores and the membrane area, i.e., with the γ factor of Eq.6. Hence the effective pore size (A_{eff}) can be estimated and it is found to be slightly lower (higher) than 1.2 \AA^2 for ${}^4\text{He}$ (${}^3\text{He}$). Finally, the behavior below threshold is shown in the inset of Fig. 2.a), where it can be seen that the probabilities

decrease exponentially as energy decreases. There the black arrow indicates the potential barrier. Nearly below this energy ^3He transmission becomes more probable, in agreement with previous 1D calculations^{11,22} where, below the barrier, the lighter atom exhibits a larger tunneling probability.

Rate coefficients as functions of temperature are determined from these probabilities (Eq.3) and the result for ^3He is presented in Fig.2.b). This WP3D rate coefficient is compared with that previously reported within TST²² except that in this work we additionally include the correction given γ (Eqs. 4 and 6). To that end, we have computed A_{eff} from the ground state TS wave function, $\Psi_0(x, y)$, as the region where $|\Psi_0(x, y)|^2$ is larger than a given cutoff, f_{cut} . Taking $f_{cut} = 10^{-4}$ leads to $\gamma(TST) = 0.033$ and 0.029 for ^3He and ^4He , respectively, a result that nicely matches the values of the probabilities mentioned above for the two isotopic species. With this choice WP3D and TST rate coefficients agree very well along the whole temperature range, except at the lowest temperatures where the WP3D coefficients are somewhat larger, probably due to an underestimation of tunneling from TST. For ^4He (no shown) WP3D and TST comparison is even more successful. Finally, the $^4\text{He}/^3\text{He}$ selectivity (ratio of rate coefficients) is reported in the inset of Fig.2.b). It can be seen that there is a fairly good agreement between the WP3D and TST calculations, although below 40 K WP3D calculations show that the preference for the transport of the heavier isotope is not as significant as originally predicted by TST.

WP3D calculations confirm the conclusions previously drawn from the TST calculations:²² both tunneling and zero point energy are very important effects in the permeability of He at low temperatures but, as they operate in opposite directions, in the end we cannot achieve a large difference between the transmission rates of the two isotopes. We would like to stress that neglect of one or the other quantum effect in the model would have led to qualitatively erroneous results. Moreover, the very low values of the related rate coefficients (Fig. 2.b)) suggest that the actual flux of these species through the sieve would be extremely slow. It is well known that permeability usually decreases as selectivity increases.⁴⁶ As a

possible strategy for achieving isotope separation, new membranes could be designed where one of the two competing quantum effects are suppressed while the flux of the more permeable species is kept sufficiently large. With that aim, we report below results for a model system where tunneling is in principle absent.

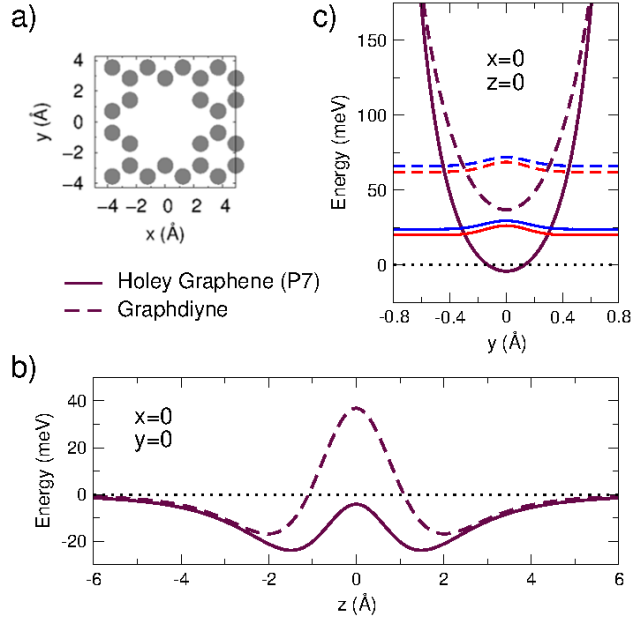


Figure 3: a) unit cell of the holey graphene model (P7) membrane. b) He-P7 interaction potential along the minimum energy path for transmission, compared with He-graphdiyne. c) also compared with He-graphdiyne, He-P7 “in-pore” interaction potential (displacement along the y coordinate for $x = 0$, $z = 0$) and profiles of the ground states at the TS for both He isotopes.

Transmission of He isotopes through a holey graphene model (P7). We have adopted the model of Sun *et al.*,³¹ where nanopores are generated by eliminating atoms from a graphene sheet and a simple Lennard-Jones pairwise interaction is assumed between He and all the carbon atoms of the membrane. Here we have chosen the same pairwise potential ($\sigma = 2.971$ Å and well depth $\epsilon = 1.611$ meV) and a membrane where the pores are created by periodically removing seven rings from graphene. The unit cell of this membrane, which will be called “P7 membrane”, is depicted in Fig.3.a). Also in that figure the main features of the He-P7 interaction are compared with those of He-graphdiyne. On the one hand and in contrast with graphdiyne (Fig.3.b)), there is not a potential barrier along the minimum

energy path of He-P7. On the other hand (Fig.3.c)) and now in similarity with the previous membrane, the difference between the ZPEs of ^4He and ^3He is considerable (4 meV). Using TST arguments, one can expect a large $^4\text{He}/^3\text{He}$ selectivity due to this difference as well as the suppression of tunneling which would favor ^3He . Interestingly, as these TS energies are much lower than those of He-graphdiyne, we foresee that the transmission rates will be much larger in the present system.

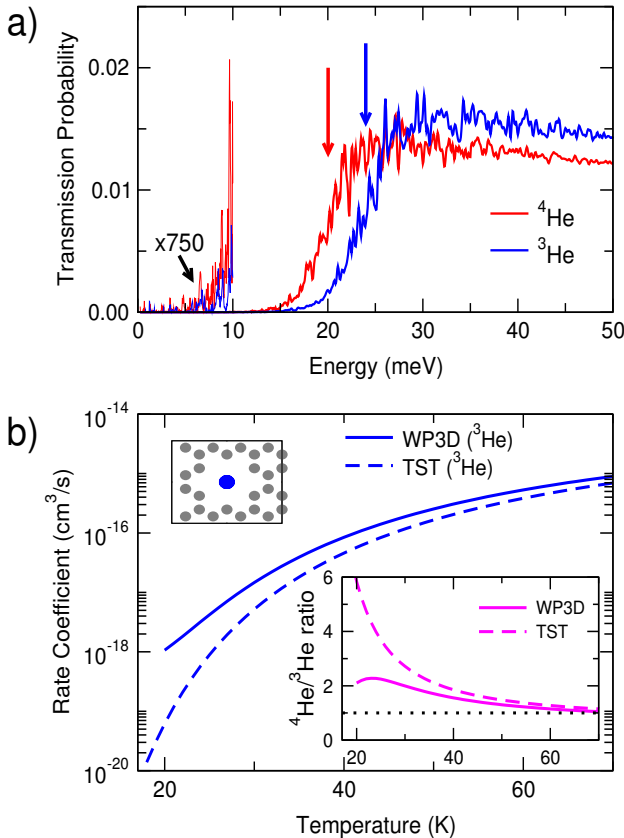


Figure 4: a) transmission probabilities of ^4He and ^3He through the P7 membrane vs. kinetic energy of the atom. Red (blue) arrow indicates the ^4He (^3He) transmission threshold as predicted by TST. For energies below 10 meV probabilities are shown magnified by a factor of 750. b) ^3He WP3D rate coefficients vs. temperature compared with TST estimations. P7 unit cell, including the TST effective area for ^3He transmission, are displayed in the upper-left inset. Finally, the $^4\text{He}/^3\text{He}$ selectivity vs. temperature is presented in the lower-right inset.

He-P7 transmission probabilities are presented in Fig.4.a). As expected, the probabilities rise at translational energies close to the TST prediction given by the TS ground state level

(20 and 24 meV for ^4He and ^3He , respectively). However and in contrast to He-graphdiyne, probabilities exhibit a multitude of peaks along the whole energy range. We have checked that these structures are not due to any artifact in the calculations. We believe that these peaks correspond to selective adsorption resonances, a process that can be understood as a temporal trapping of the incident wave into a bound state of the laterally averaged potential while the motion along the parallel coordinates, ruled by the Bragg condition, becomes faster for the sake of the conservation of energy.³²⁻³⁴ Analysis of the wave packet propagation supports this argument: it is noticed that after the main portion of the wave packet has been either reflected or transmitted by direct scattering, a non-negligible fraction of this wave packet remains trapped along the adsorption region ($\approx 3 \text{ \AA}$) for a long time while it is slowly decaying towards the reflection or the transmission regions. Resonance structures are not seen in the He-graphdiyne transmission probabilities probably because they are extremely narrow. We plan to further study the role played by these resonances from simulations of the decaying of initially prepared adsorbed states.³⁴

WP3D rate coefficients for ^3He -P7 as functions of temperature are reported in Fig.4.b). Comparing with graphdiyne (Fig.2.b)), it is worth noticing their large absolute values which are due to the lower thresholds in the transmission probabilities. TST calculations have been also performed for this system to test whether this theory can predict the WP3D results. TST rate coefficients were obtained using Eq. 4 where, in this case, $f_{tunn} = 1$, as the minimum energy path is barrier-less. The γ factor has been computed, as for graphdiyne, from the TS ground state wave function and taking the same value for f_{cut} . The results are $\gamma(TST) = 0.0130$ and 0.0144 for ^3He and ^4He , respectively, which are in fairly good agreement with the heights of the plateaus reached for the probabilities in the higher energy region (Fig.4.a)). However, TST rate coefficients do not agree quite well with the WP3D calculations, especially at low temperatures where differences become of almost two orders of magnitude. TST also underestimates the rate coefficients of ^4He -P7 (not shown) although to a lesser extent. As a consequence, TST is unable to predict the qualitative behavior of the

$^4\text{He}/^3\text{He}$ selectivity ratio, reported in the inset of Fig.4.b). In fact, while TST predicts an increase of the $^4\text{He}/^3\text{He}$ selectivity as temperature decreases (reaching a promising value of six at 20 K), the accurate treatment gives a maximum of just 2.3 at about 23 K. Tunneling along non minimum energy paths (either direct or mediated by the resonances⁴⁷) can be at the origin of the larger values of the WP3D rate coefficients. The fact that discrepancies are larger for the lighter isotope supports this argument. Therefore, it appears that tunneling still operates for this system and competes with ZPE effects so that, after all, the quantum sieving is not as important as initially expected based on simpler theories.

Conclusion. We have reported an accurate three-dimensional wave packet approach for the study of the passage of atoms through nanoporous one-atom-thick membranes. Results of simulations of the transmission of He isotopes through graphdiyne and a leaky graphene model indicate the relevance of quantum effects such as tunneling, transition state zero point energy and, as a novelty, resonances. Transition state theory is found to be successful for He-graphdiyne but fails for the holey graphene model. This approach can be used as a reference in studies of the range of validity of this and other approximate theories. Furthermore, it is possible to extend this method to more complex systems such as diatoms or bilayered membranes, for instance. We plan to work along some of these lines in the near future.

Supporting Information

Computational details of the three-dimensional wave packet calculations for the transmission of atoms through periodic membranes.

Acknowledgments

We thank Dr. Massimiliano Bartolomei for helpful discussions and a critical reading of the manuscript. The work has been funded by Spanish MINECO grant FIS2013-48275-C2-1-P.

Allocation of computing time by CESGA (Spain) and support by the COST-CMTS Action CM1405 “Molecules in Motion (MOLIM)” are also acknowledged.

References

- (1) Koenig, S. P.; Wang, L.; Pellegrino, J.; Bunch, J. S. Selective Molecular Sieving through Porous Graphene. *Nature Nanotechnology* **2012**, *7*, 728–732.
- (2) Jiao, Y.; Du, A.; Hankel, M.; Smith, S. C. Modelling Carbon Membranes for Gas and Isotope Separation. *Phys. Chem. Chem. Phys.* **2013**, *15*, 4832–4843.
- (3) Huang, L.; Zhang, M.; Li, C.; Shi, G. Graphene-Based Membranes for Molecular Separation. *J. Phys. Chem. Lett.* **2015**, *6*, 2806–2815.
- (4) Schrier, J. Helium Separation Using Porous Graphene Membranes. *J. Phys. Chem. Lett.* **2010**, *1*, 2284–2287.
- (5) Hauser, A. W.; Schwerdtfeger, P. Nanoporous Graphene Membranes for Efficient $^3\text{He}/^4\text{He}$ Separation. *J. Phys. Chem. Lett.* **2012**, *3*, 209–213.
- (6) Cho, A. Helium-3 Shortage Could Put Freeze on Low-Temperature Research. *Science* **2009**, *326*, 778–779.
- (7) Nuttall, W. J.; Clarke, R. H.; Glowacki, B. A. Resources: Stop Squandering Helium. *Nature* **2012**, *485*, 573–575.
- (8) Cai, J.; Xing, Y.; Zhao, X. Quantum Sieving: Feasibility and Challenges for the Separation of Hydrogen Isotopes in Nanoporous Materials. *RSC Advances* **2012**, *2*, 8579–8586.
- (9) Hauser, A. W.; Schrier, J.; Schwerdtfeger, P. Helium Tunneling through Nitrogen-Functionalized Graphene Pores: Pressure- and Temperature-Driven Approaches to Isotope Separation. *J. Phys. Chem. C* **2012**, *116*, 10819–10827.

- (10) Mandrà, S.; Schrier, J.; Ceotto, M. Helium Isotope Enrichment by Resonant Tunneling through Nanoporous Graphene Bilayers. *J. Phys. Chem. A* **2014**, *118*, 6457–6465.
- (11) Bartolomei, M.; Carmona-Novillo, E.; Hernández, M. I.; Campos-Martínez, J.; Pirani, F.; Giorgi, G. Graphdiyne Pores: "Ad Hoc" Openings for Helium Separation Applications. *J. Phys. Chem. C* **2014**, *118*, 29966–29972.
- (12) Lalitha, M.; Lakshmipathi, S.; Bhatia, S. K. Defect-Mediated Reduction in Barrier for Helium Tunneling through Functionalized Graphene Nanopores. *J. Phys. Chem. C* **2015**, *119*, 20940–20948.
- (13) Li, F.; Qu, Y.; Zhao, M. Efficient Helium Separation of Graphitic Carbon Nitride Membrane. *Carbon* **2015**, *95*, 51–57.
- (14) Qu, Y.; Li, F.; Zhou, H.; Zhao, M. Highly Efficient Quantum Sieving in Porous Graphene-like Carbon Nitride for Light Isotopes Separation. *Scientific Reports* **2016**, *6*, 19952.
- (15) Beenakker, J. J. M.; Borman, V. D.; Krylov, S. Y. Molecular Transport in Subnanometer Pores: Zero-Point Energy, Reduced Dimensionality and Quantum Sieving. *Chem. Phys. Lett.* **1995**, *232*, 379–382.
- (16) We employ the term "ZPE effects" to refer in general to the effects due to the quantization of the states within the pore (identified as the transition state), and more specifically, to the in-pore ground state as it is the most populated state at low temperatures.
- (17) Hankel, M.; Zhang, H.; Nguyen, T. X.; Bhatia, S. K.; Gray, S. K.; Smith, S. C. Kinetic Modelling of Molecular Hydrogen Transport in Microporous Carbon Materials. *Phys. Chem. Chem. Phys.* **2011**, *13*, 7834–7844.

- (18) Kumar, A. V. A.; Bathia, S. K. Quantum Effect Induced Reverse Kinetic Molecular Sieving in Microporous Materials. *Phys. Rev. Lett.* **2005**, *95*, 245901.
- (19) Schrier, J.; McClain, J. Thermally-Driven Isotope Separation across Nanoporous Graphene. *Chem. Phys. Lett.* **2012**, *521*, 118–124.
- (20) Zhao, X.; Villar-Rodil, S.; Fletcher, A. J.; Thomas, K. M. Kinetic Isotope Effect for H₂ and D₂ Quantum Molecular Sieving in Adsorption/Desorption on Porous Carbon Materials. *J. Phys. Chem. B* **2006**, *110*, 9947–9955.
- (21) Nguyen, T. X.; Jobic, H.; Bathia, S. K. Microscopic Observation of Kinetic Molecular Sieving of Hydrogen Isotopes in a Nanoporous Material. *Phys. Rev. Lett.* **2010**, *105*, 085901.
- (22) Hernández, M. I.; Bartolomei, M.; Campos-Mertínez, J. Transmission of Helium Isotopes through Graphdiyne Pores: Tunneling versus Zero Point Energy Effects. *J. Phys. Chem. A* **2015**, *119*, 10743–10749, (Note that, the rate coefficients computed and shown in Fig. 4 therein were erroneously multiplied by $(2\pi)^{-3/2}$. This error does not affect either the rest of the results nor the conclusions of the work.).
- (23) Li, G.; Li, Y.; Liu, H.; Guo, Y.; Li, Y.; Zhu, D. Architecture of Graphdiyne Nanoscale Films. *Chem. Commun.* **2010**, *46*, 3256–3258.
- (24) Zhou, J.; Gao, X.; Liu, R.; Xie, Z.; Yang, J.; Zhang, S.; Zhang, G.; Liu, H.; Li, Y.; Zhang, J.; Liu, Z. Synthesis of Graphdiyne Nanowalls Using Acetylenic Coupling Reaction. *J. Am. Chem. Soc.* **2015**, *137*, 7596–7599.
- (25) Jiao, Y.; Du, A.; Hankel, M.; Zhu, Z.; Rudolph, V.; Smith, S. C. Graphdiyne: A Versatile Nanomaterial for Electronics and Hydrogen Purification. *Chem. Commun.* **2011**, *47*, 11843–11845.
- (26) Cranford, S. W.; Buehler, M. J. Selective Hydrogen Purification through Graphdiyne under Ambient Temperature and Pressure. *Nanoscale* **2012**, *4*, 4587–4593.

- (27) Bartolomei, M.; Carmona-Novillo, E.; Hernández, M. I.; Campos-Martínez, J.; Pirani, F.; Giorgi, G.; Yamashita, K. Penetration Barrier of Water through Graphynes' Pores: First-Principles Predictions and Force Field Optimization. *J. Phys. Chem. Lett.* **2014**, *5*, 751–755.
- (28) Balakrishnan, N.; Kalyanaraman, C.; Sathyamurthy, N. Time-Dependent Quantum Mechanical Approach to Reactive Scattering and Related Processes. *Phys. Rep.* **1997**, *280*, 79–144.
- (29) Balint-Kurti, G. G. Time-Dependent and Time-Independent Wavepacket Approaches to Reactive Scattering and Photodissociation Dynamics. *Int. Rev. Phys. Chem.* **2008**, *27*, 507–539.
- (30) Yinnon, A. T.; Kosloff, R. A Quantum-Mechanical Time-Dependent Simulation of the Scattering from a Stepped Surface. *Chem. Phys. Lett.* **1983**, *102*, 216–223.
- (31) Sun, C.; Boutilier, M. S. H.; Au, H.; Poesio, P.; Bai, B.; Karnik, R.; Hadjiconstantinou, N. G. Mechanisms of Molecular Permeation through Nanoporous Graphene Membranes. *Langmuir* **2014**, *30*, 675–682.
- (32) Lennard-Jones, J. E.; Devonshire, A. F. Diffraction and Selective Adsorption of Atoms at Crystal Surfaces. *Nature* **1936**, *137*, 1069–1070.
- (33) Sanz, A. S.; Miret-Artés, S. Selective Adsorption Resonances: Quantum and Stochastic Approaches. *Physics Reports* **2007**, *451*, 37–154.
- (34) Hernández, M. I.; Campos-Martínez, J.; Miret-Artés, S.; Coalson, R. D. Lifetimes of Selective-Adsorption Resonances in Atom-Surface Elastic Scattering. *Phys. Rev. B* **1994**, *49*, 8300–8309.
- (35) Feit, M. D.; Fleck, J. A.; Steiger, A. Solution of the Schrödinger Equation by a Spectral Method. *J. Comput. Phys.* **1982**, *47*, 412–433.
- (36) Kosloff, D.; Kosloff, R. A Fourier Method Solution for the Time Dependent Schrödinger Equation as a Tool in Molecular Dynamics. *J. Comp. Phys.* **1983**, *52*, 35–53.
- (37) Heller, E. J. Time-Dependent Approach to Semiclassical Dynamics. *J. Chem. Phys.* **1975**, *62*, 1544–1555.

- (38) Pernot, P.; Lester, W. A. Multidimensional Wave-Packet Analysis: Splitting Method for Time-Resolved Property Determination. *Int. J. Quantum Chem.* **1991**, *40*, 577–588.
- (39) Miller, W. H. Quantum Mechanical Transition State Theory and a New Semiclassical Model for Reaction Rate Constants. *J. Chem. Phys.* **1974**, *61*, 1823–1834.
- (40) Zhang, D.; Zhang, J. Z. H. Full-Dimensional Time-Dependent Treatment for Diatom-Diatom Reactions: The H₂+OH Reaction. *J. Chem. Phys.* **1991**, *101*, 1146–1156.
- (41) di Domenico, D.; Hernández, M. I.; Campos-Martínez, J. A Time-Dependent Wave Packet Approach for Reaction and Dissociation in H₂+H₂. *Chem. Phys. Lett.* **2001**, *342*, 177–184.
- (42) Truhlar, D. G.; Kuppermann, A. Exact and Approximate Quantum Mechanical Reaction Probabilities and Rate Constants for the Collinear H + H₂ Reaction. *J. Chem. Phys.* **1972**, *56*, 2232–2252.
- (43) Garret, B. C.; Truhlar, D. G. Accuracy of Tunneling Corrections to Transition State Theory for Thermal Rate Constants of Atom Transfer Reactions. *J. Phys. Chem.* **1979**, *83*, 200–203.
- (44) Wang, Y.; Li, J.; Yang, Q.; Zhong, C. Two-Dimensional Covalent Triazine Framework Membrane for Helium Separation and Hydrogen Purification. *ACS Appl. Mater. Interfaces* **2016**, *8*, 8694–8701.
- (45) Pirani, F.; Brizi, S.; Roncaratti, L.; Casavecchia, P.; Cappelletti, D.; Vecchiocattivi, F. Beyond the Lennard-Jones Model: A Simple and Accurate Potential Function Probed by High Resolution Scattering Data Useful for Molecular Dynamics Simulations. *Phys. Chem. Chem. Phys.* **2008**, *10*, 5489–5503.
- (46) Robeson, L. M. The Upper Bound Revisited. *J. Membrane Sci.* **2008**, *320*, 390–400.
- (47) Liu, K. Quantum Dynamical Resonances in Chemical Reactions: from A+BC to Polyatomic Systems. *Adv. Chem. Phys.* **2012**, *149*, 1–46.